One- and Two-Dimensional Maximum Softening Indicators for Reinforced Concrete Structures under Seismic Excitation

Nielsen, Søren R. K.; Köyüoglu, H. U.; Cakmak, A. S.

Publication date:
1992

Document Version
Publisher's PDF, also known as Version of record

INSTITUTTET FOR BYGNINGSTEKNIK
DEPT. OF BUILDING TECHNOLOGY AND STRUCTURAL ENGINEERING
AALBORG UNIVERSITETSCENTER • AUC • AALBORG • DANMARK

STRUCTURAL RELIABILITY THEORY
PAPER NO. 92

S. R. K. NIELSEN, H. U. KÖYLÜOĞLU & A. Ş. ÇAKMAK

ONE AND TWO-DIMENSIONAL MAXIMUM SOFTENING DAMAGE INDICATORS FOR REINFORCED CONCRETE STRUCTURES UNDER SEISMIC EXCITATION

JUNE 1992 ISSN 0902-7513 R9211

INSTITUTTET FOR BYGNINGSTEKNIK
DEPT. OF BUILDING TECHNOLOGY AND STRUCTURAL ENGINEERING
AALBORG UNIVERSITETSCENTER • AUC • AALBORG • DANMARK

STRUCTURAL RELIABILITY THEORY
PAPER NO. 92

S. R. K. NIELSEN, H. U. KÖYLÜOĞLU & A. Ş. ÇAKMAK

ONE AND TWO-DIMENSIONAL MAXIMUM SOFTENING DAMAGE INDICATORS FOR REINFORCED CONCRETE STRUCTURES UNDER SEISMIC EXCITATION

JUNE 1992 ISSN 0902-7513 R9211

ONE AND TWO-DIMENSIONAL MAXIMUM SOFTENING DAMAGE INDICATORS FOR REINFORCED CONCRETE STRUCTURES UNDER SEISMIC EXCITATION

S. R. K. Nielsen,[1] H. U. Köylüoğlu[2] and A. Ş. Çakmak[2]

ABSTRACT

The maximum softening concept is based on the variation of the vibrational periods of a structure during a seismic event. Maximum softening damage indicators, which measure the maximum relative stiffness reduction caused by stiffness and strength deterioration of the actual structure, are calculated for an equivalent linear structure with slowly varying stiffness characteristics. In the paper, a one dimensional scalar-valued and a two-dimensional vector-valued maximum softening damage indicator are defined. The one-dimensional damage indicator, defined considering the variation in the first period of the structure, analogous to a SDOF system, is a genuine global damage index representing the average damage throughout the whole structure. The two-dimensional damage indicator is defined considering the variations in the first and second periods, and thus is analogous to an equivalent linear two degrees-of-freedom system. The components of the damage vector can be interpreted as damage indicators for the lower half and the upper half of the structure, hence representing a simple local description of the damage state of the structure. Since statements on the post earthquake reliability should be obtained solely from knowledge of the latest recorded values of the damage indicators above defined, these are required to possess a Markov property. This problem has been investigated based on numerical Monte-Carlo simulations, and it is observed that the Markov assumption of the one-dimensional damage indicator is justified for the mean value of the transition probability density function (tpdf), whereas some deviations are observed for the variance and higher order statistical moments. For the two-dimensional damage indicator the Markov assumption seems justified for both the mean values and the covariances of the tpdf. From these, it is concluded that the Markov properties of the mean and covariances of the two-dimensional indicators are superior to the Markov property of the first and second order moments of the one-dimensional damage indicator.

1. INTRODUCTION

Local damage in reinforced concrete structures can be attributed to micro-cracking, bond deterioration at the steel-concrete interfaces and yielding of the reinforcement bars. To

[1] Department of Building Technology and Structural Engineering, University of Aalborg, DK-9000 Aalborg, Denmark

[2] Department of Civil Engineering and Operations Research, Princeton University, Princeton, NJ 08544, USA

the extent that framed reinforced concrete structures can be modeled by conventional non-linear beam theories, local damage at a cross-section of the structure can adequately be measured by the degradation of bending stiffness and moment capacity of the cross-section. In any case, the overall effect of local damage is deterioration of stiffness and strength of the structure. A global damage indicator can then be defined as a scalar or vector-valued function of such continuously distributed local damages which characterize the overall damage state and serviceability of the structure.

Global damage indicators are response quantities characterizing the damage state of the structure after earthquake excitations, and as such can be used in decision-making during the design phase or in case of post-earthquake reliability and repair problems. In serving these purposes, a global damage indicator should ideally fulfill at least the following requirements:

1. The damage indicator should be observable by measurements.
2. The damage indicator should be a non-decreasing function of time unless the structure is repaired or strengthened.
3. Dependent on the definition of the failure event, a well-defined deterministic failure surface in the space of the component damage indicators, separating safe states from unsafe states of the structure, should exist.
4. It should be possible to derive post-earthquake reliability estimates for a partly damaged structure solely from the latest recorded value of the damage indicator.

For practical purposes, the first requirement must be met so that measurements can be used to quantify global damage. The second requirement implies that a structure which is hit by an earthquake will always have an increase in at least one of the components of the damage indicator. Dependent on the functional relation between the definition of the failure event and measured damage indicator values for the failure event, the third requirement indicates the existence of a serviceability limit state.

The fourth requirement implies that two initially identical structures, for which the same present value of the scalar or vectorial global damage indicator is recorded, should be considered to have the same structural reliability, when exposed to the same future earthquake process, independent of preceding different loading histories. Mathematically, this means that the values of the global damage indicator after each earthquake are assumed to form a Markov chain. If the local damages, as measured by the stiffness and strength deterioration of all beams and columns, are point-wise the same throughout the two structures, the probability distributions of local damages certainly will be identical after the next earthquake, irrespective of the different preceding loading histories. This establishes the Markov property for the finite or infinite dimensional vector process made up of all local damage measures. A sufficient condition for this case is obtained, if the local damages have the same spatial distribution in all loading histories, so that the damage state can be described by a single scaling parameter. Then the local damage is identical in the two structures if the global damage indicators are the same. In this case the sequence of scalar global damage indicator values forms a Markov chain. On the other hand, any violation of the Markov property for the one-dimensional damage indicator can be attributed to different spatial distributions of the local damage in different loading sequences. In general, the Markov property does not apply very well to a scalar global damage indicator process. However, if the components of the vector damage indicator process can be interpreted as a measure of average damage in various part of the structure, and hence represent a crude description of local damages, a better fit to the Markov property may be expected.

The maximum softening concept is based on the variations of the vibrational periods of a structure during a seismic event. The variation in the vibrational periods is partly caused by the degradation of the incremental stiffness in the elastic range, and partly by the averaged effect of the loss of incremental stiffness at excursions into the plastic range at various positions in the structure. The maximum softening damage indicators are defined as the maximum relative stiffness reduction caused by stiffness and strength deterioration. The numerical values for the damage indicators are calculated, dependent on the variation in the vibrational periods, for an equivalent linear system with slowly varying stiffness characteristics.

The one-dimensional maximum softening concept based on an equivalent linear SDOF system was introduced by DiPasquale and Cakmak (1987) as a global damage indicator for reinforced concrete structures. This index is calibrated based on an analysis of data from shake table experiments with reinforced concrete frames performed by Sozen and his associates at the University of Illinois at Urbana Champaign in the 1970's (Healey and Sozen (1978), Cecen (1979)). It was demonstrated that the maximum softening values at failure showed relatively small variability independently of the limit state definition, which ranged from slightly damped structures to total collapse. Hence the one-dimensional maximum softening damage indicator fulfills the third of the indicated requirements within acceptable limits. A comparison of the one-dimensional maximum softening with other global damage indicators showed the versatility of the maximum softening in separating failed from unfailed structures was further demonstrated by Rodriquez-Gomez (1990). Nielsen and Cakmak (1991) investigated the Markov property of the sequence of one-dimensional maximum softening values based on Monte-Carlo simulations using the SARCF-II program (Rodriguez-Gomez et al. (1990)), and found that the Markov property was fulfilled for the mean value of the transitional probability density, but that deviations were observed for higher order conditional moments. Because of the inability of the applied structural analysis program to handle severely damaged structures, the considered samples might have been biased to some extent. For this reason this analysis will also be re-iterated in the present study with a robust structural analysis program SARCOF developed by Mørk (1992).

In the present study, a generalization of the one-dimensional maximum concept to two dimensions has been suggested, where the components of the damage indicator can be interpreted as the maximum softening of, respectively, the lower and the upper half of the structure. Hence, the two-dimensional maximum softening provides a simple and crude description of the distribution of damages in the structure.

The Markov property of the one-dimensional and the two-dimensional maximum softening damage indicators is tested numerically by means of Monte Carlo simulation. In doing this, the earthquake surface acceleration process is modelled as the response from an intensity modulated Gaussian white noise, filtered through a Kanai-Tajimi filter. Structural analysis is performed with the computer program SARCOF, which has been especially developed for stochastic analysis of reinforced concrete frames under seismic excitation based on Monte-Carlo simulations. The theoretical background and the capabilities of this program are given in Mørk (1992). The program considers moment-curvature relation as an extended version of the model developed by Roufaiel-Meyer (1987), taking into account the transition from uncracked to cracked sections. Strength deterioration is assumed to be related to crushing of concrete in the compression zone, and is functionally correlated to the hysteretic energy accumulated in the cross-section subsequent to the first exceedance of a critical curvature. The finite length of plastic zones is taken into account, controlling the plasticity at the end sections and at 3 internal cross-sections. The incremental bending stiffness field is next obtained by linear interpolation between the value at these sections. Finally, a system reduction scheme, based on a truncated expansion of external nodal point degrees-of-freedom, in the linear eigenmodes of the initial undamaged structure has been implemented. However, a full description is maintained of the internal degrees-of-freedom, controlling the hysteresis at the control sections.

2. MAXIMUM SOFTENING DAMAGE INDICATORS

Figure 1a shows the time-variation of the first and second eigenperiod of the structure during the ith earthquake, initiated at the time t_i and of the length l_i. Both time-series have been normalized with respect to the corresponding eigenperiods $T_1(0)$ and $T_2(0)$ of the initial referential state, where the structure is exposed to gravity loads alone. Partial cracking of the cross-sections due to gravity loads has been considered at the evaluation of $T_1(0)$ and $T_2(0)$. The increase of the eigenperiods from the value $T_j(t_i)$, $j = 1,2$ at the start of the ith earthquake to the final value $T_j(t_i + l_i)$, $j = 1,2$ at the end of the excitation can be attributed to the gradual deterioration of incremental bending stiffness at elastic branches of the moment-curvature relations. The local peaks of the eigenperiod time-series are caused by the complete loss of incremental stiffness during momentary excursions into the plastic range. In Figure 1a, the moving time-averages $\hat{T}_j(t_i)$, $j = 1,2$ of the eigenperiod time-series are also shown. As suggested by Rodriguez-Gomez (1990), these time-averages may be identified as the eigenperiods of the equivalent linear systems with slowly varying parameters as shown in Figure 1b and Figure 1c. Due to the plastic deformations, $\hat{T}_j(t_i)$, $j = 1,2$ attains a maximum value during the ith earthquake at the instants of time $t_{j,i}$, $j = 1,2$. In general $t_{1,i} \neq t_{2,i}$ as also is the case in Figure 1a.

The one-dimensional maximum softening damage indicator is then defined as follows (DiPasquale and Cakmak (1987, 1990))

$$D_{0,i} = 1 - \left(\frac{\hat{k}_0(t_{1,i})}{k_0(0)}\right)^{\frac{1}{2}} = 1 - \frac{T_1(0)}{\hat{T}_1(t_{1,i})} \tag{1}$$

where $\hat{k}_0(t)$ and $k_0(0)$ signify the spring constant of the equivalent linear SDOF system in Figure 1b at the time t, and the corresponding spring constant at $t = 0$ for the initial undamaged structure.

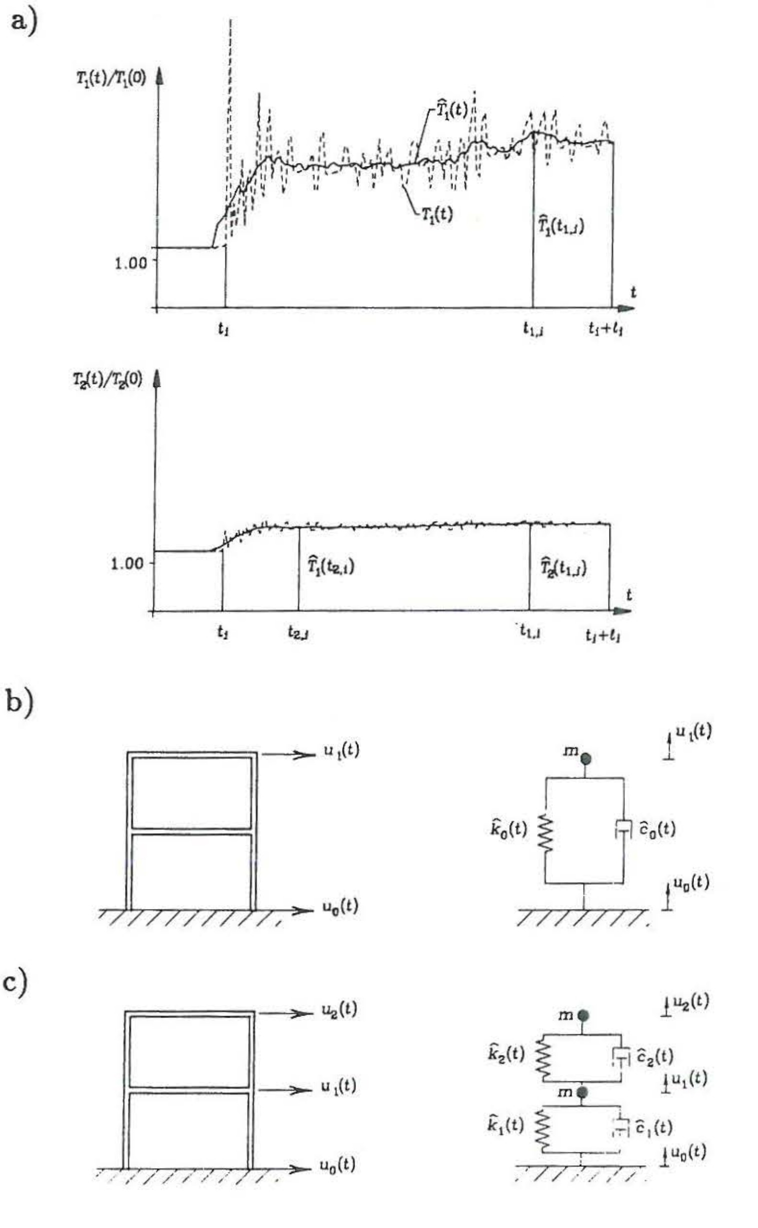

Fig. 1: a) Time-variation of first and second eigenperiods. b) Equivalent linear SDOF system. c) Equivalent linear two-degrees-of-freedom system.

In Figure 1c, a generalization of this concept is shown, where the structure is replaced by an equivalent linear two-degrees-of-freedom system. The time-dependent spring constants of the equivalent system represent, respectively, the equivalent stiffness of the lower half and the upper half of the structure. The masses of the equivalent linear system are assumed to be of equal magnitude m. The following damage indicators can then be introduced, indicating respectively the maximum softening after the ith earthquake of the lower half and the upper half of the structure

$$D_{j,i} = 1 - \left(\frac{\hat{k}_j(t_{1,i})}{k_j(0)} \right)^{\frac{1}{2}}, \quad j = 1,2 \tag{2}$$

where $\hat{k}_1(t_{1,i})$ and $\hat{k}_2(t_{1,i})$ signify the spring constants of the equivalent linear system at the instant of time $t_{1,i}$, where the one-dimensional maximum softening $D_{0,i}$ in the ith earthquake occurs. Because the initial values $k_0(0)$, $k_1(0)$ and $k_2(0)$ of the equivalent spring constants are needed in the definitions, both the one-dimensional and the two-dimensional maximum softening indicator require that the structure has been instrumented from its construction. The following quantities are introduced to define spring constants

$$\hat{\omega}_j = \frac{2\pi}{\hat{T}_j(t_{1,i})}, \quad j = 1, 2 \tag{3}$$

Notice, that $\hat{\omega}_2$ has been defined from $\hat{T}_2(t_{1,i})$ rather than from $\hat{T}_2(t_{2,i})$. $\hat{k}_1(t_{1,i})$ and $\hat{k}_2(t_{1,i})$ can then be identified from the following expressions, derived from the solutions to the characteristic equation of the equivalent linear two-degrees-of-freedom system

$$\frac{\hat{k}_1(t_{1,i})}{m} = \frac{1}{2}\left(\hat{\omega}_1^2 + \hat{\omega}_2^2 - \sqrt{\hat{\omega}_1^4 - 6\hat{\omega}_1^2\hat{\omega}_2^2 + \hat{\omega}_2^4}\,\right) \tag{4}$$

$$\frac{\hat{k}_2(t_{1,i})}{m} = \frac{1}{4}\left(\hat{\omega}_1^2 + \hat{\omega}_2^2 + \sqrt{\hat{\omega}_1^4 - 6\hat{\omega}_1^2\hat{\omega}_2^2 + \hat{\omega}_2^4}\,\right) \tag{5}$$

(4) and (5) can only be used, if $\hat{\omega}_2 \geq \sqrt{3+\sqrt{8}}\,\hat{\omega}_1$. If $\hat{\omega}_2 < \sqrt{3+\sqrt{8}}\,\hat{\omega}_1$, the following expressions are used instead

$$\frac{\hat{k}_1(t_{1,i})}{m} = \frac{1}{2}\left(\hat{\omega}_1^2 + \hat{\omega}_2^2\right) \tag{6}$$

$$\frac{\hat{k}_2(t_{1,i})}{m} = \frac{1}{4}\left(\hat{\omega}_1^2 + \hat{\omega}_2^2\right) \tag{7}$$

3. LIMIT SURFACES FOR MAXIMUM SOFTENING DAMAGE INDICATORS

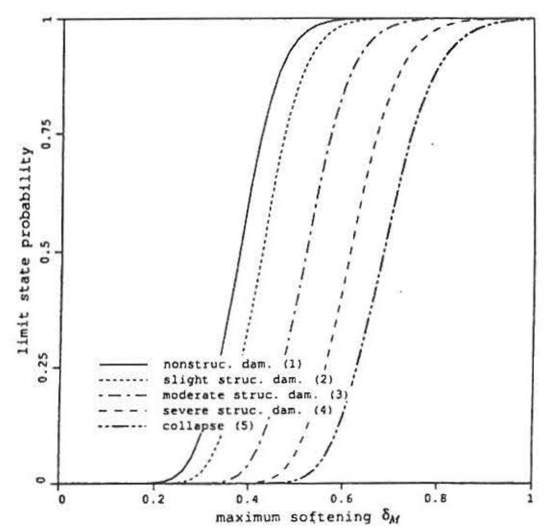

Fig. 2: Distribution of observed limit state values of one-dimensional maximum softening (DiPasquale and Cakmak (1989)).

In Figure 2, the distribution function of observed values of the one-dimensional maximum softening, obtained from analysis of shake table experiments with reinforced concrete frames (Healey and Sozen (1978), Cecen (1979)), is shown. The limit state definition varied from insignificant damage to total collapse. In all cases a relatively small variational coefficient was observed for the damage indicator. From this analysis it is concluded that safe states of the structure can be separated from unsafe states with sufficient reliability, by determining whether or not the maximum softening D_0 exceeds a critical value d_0. The failure event is then defined by $\{D_0 \geq d_0\}$.

For the two-dimensional damage indicator, the corresponding failure surface in the sample space of the damage indicators D_1 and D_2 can be explicitly derived from the solution for ω_1^2 of the characteristic equation. Using (1), (2) the failure surface can be determined from the following relations

$$d_2 = 1 - \sqrt{\frac{1}{4\lambda}}\sqrt{\frac{\delta^2 - 2\delta(1-d_1)^2}{\delta - (1-d_1)^2}}, \qquad 0 \leq d_1 \leq d_{1,\max} \tag{8}$$

$$\lambda = \frac{k_2(0)}{k_1(0)} \tag{9}$$

$$\delta = (1-d_0)^2\left(1 + 2\lambda - \sqrt{1+4\lambda^2}\,\right) \tag{10}$$

$$d_{1,\max} = 1 - \sqrt{\frac{4\lambda\delta - \delta^2}{4\lambda - 2\delta}} \tag{11}$$

d_2 as determined by (8) is monotonously decreasing in the interval of definition from the maximum value $d_{2,\max} = 1 - \sqrt{\frac{1}{4\lambda}}\sqrt{\frac{\delta^2-2\delta}{\delta-1}}$ at $d_1 = 0$ to $d_2 = 0$ at $d_1 = d_{1,\max}$. A plot of the functional relation (8) is shown in Figure 3.

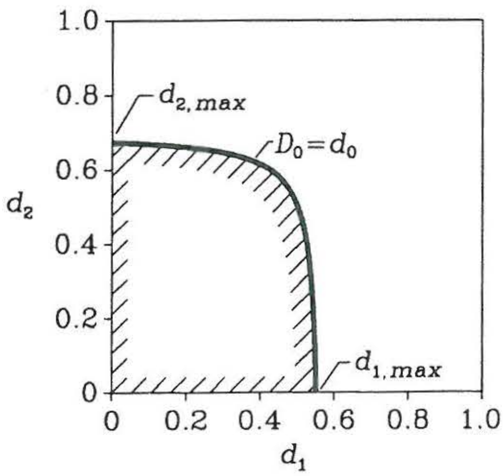

Fig. 3: Failure surface for two-dimensional maximum softening damage indicator. $\lambda = 1.00$, $d_0 = 0.50$.

4. TEST OF MARKOV PROPERTY OF DAMAGE INDICATORS

The maximum softening damage indicators fulfill the first and second indicated requirements as well as the third requirement, with sufficient reliability. In what follows, the fourth requirement, the Markov property of the damage indicator sequences will be tested.

The Markov property of the sequences of maximum softening values $\{D_{0,i}, i = 1,2,\ldots\}$ and $\{\mathbf{D}_i, i = 1,2,\ldots\}$, $\mathbf{D}_i^T = [D_{1,i}, D_{2,i}]$ can equivalently be tested from the following conditional joint moment relations

$$\forall k,i \quad : \quad E[D_{0,i}^k \mid D_{0,i-1} = d_{0,i-1},\ldots,D_{0,1} = d_{0,1}] = E[D_{0,i}^k \mid D_{0,i-1} = d_{0,i-1}] \tag{12}$$

$$\forall k,l,i \quad : \quad E[D_{1,i}^k D_{2,i}^l \mid \mathbf{D}_{i-1} = \mathbf{d}_{i-1},\ldots,\mathbf{D}_1 = \mathbf{d}_1] = E[D_{1,i}^k D_{2,i}^l \mid \mathbf{D}_{i-1} = \mathbf{d}_{i-1}] \tag{13}$$

The order k and $k+l$ for which (12) and (13) are valid will be tested empirically by means of Monte Carlo simulation. If the damage indicator sequences possess the Markov property, they must satisfy the above criteria listed in (12) and (13) for arbitrary k and $k+l$.

5. NUMERICAL RESULTS

The considered structure for numerical study is the planar 3 story 2 bay reinforced concrete frame shown on fig. 4, which has been designed according to the UBC specifications for earthquake zone 4. The geometrical and structural details of the frame are indicated on the figure. The linear first and second eigenperiods of the undamaged structure are $T_1(0)$ =0.493 s and $T_2(0)$ =0.168 s, corresponding to the initial angular eigenfrequencies $\omega_1(0)$ =12.74 s^{-1} and $\omega_2(0)$ =37.4 s^{-1}.

This structure is excited by a horizontal acceleration process at the ground surface, which is determined as the response process of an intensity modulated Gaussian white noise, filtered through a Kanai-Tajimi filter with parameters ω_0 and ζ_0 (Tajimi (1960)).

The bedrock acceleration process $\{\ddot{r}_b(t),\ t \in [0,\infty)\}$ is modeled as a time modulated unit Gaussian white noise process, i.e.

$$\ddot{r}_b(t) = \beta(t)W(t) \tag{14}$$

$\{W(t),\ t \in [0,\infty)\}$ is a unit white noise process, which is a zero mean Gaussian process with the auto-covariance function

$$E[W(t_i)W(t_j)] = \delta(t_i - t_j) \tag{15}$$

where $\delta(\cdot)$ is the Dirac delta-function. Realizations of a unit Gaussian white noise process are generated by the method of Ruiz and Penzien (1969).

$\beta(t)$ is a deterministic intensity function, defined as (Jennings et al. (1968))

$$\beta(t) = \beta_0 \cdot \begin{cases} \frac{t^2}{t_1^2} & , \quad 0 \le t \le t_1 \\ 1 & , \quad t_1 < t < t_0 + t_1 \\ \exp\big(-c(t - t_0 - t_1)\big) & , \quad t_0 + t_1 \le t \end{cases} \tag{16}$$

where β_0 is a given amplitude.

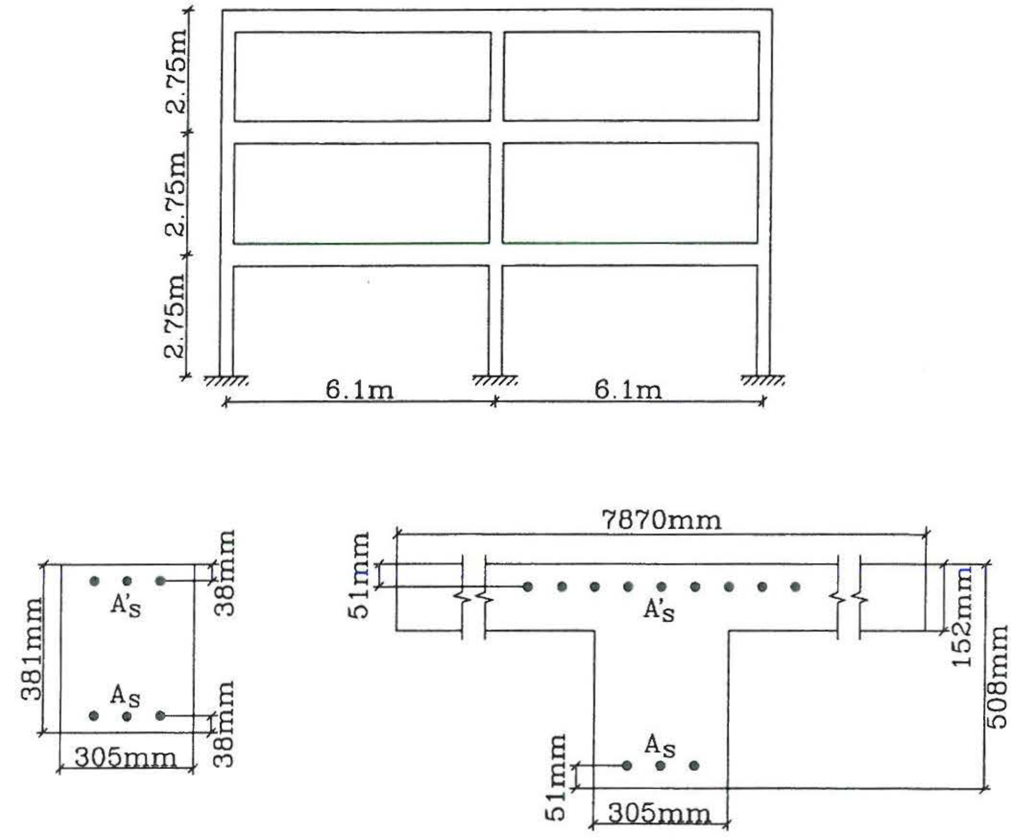

$A'_S = 1.64 \cdot 10^{-3}\, m^2$
$A_S = 1.64 \cdot 10^{-3}\, m^2$

Column

$A'_S = 1.64 \cdot 10^{-3}\, m^2$
$A_S = 1.14 \cdot 10^{-3}\, m^2$

Beam

$\rho = 2500 kg/m^3$, $E_C = 3.50 \cdot 10^{10}$ Pa , $\sigma_C = 27.6$ MPa , $\sigma_{s,y} = 414$ MPa

Fig. 4: Details of 3 story 2 bay reinforced concrete frame, UBC zone 4. (Rodriquez-Gomez (1990)).

Application of the Kanai-Tajimi filter implies, that the displacement of the earth surface $r_0(t)$ relative to the bedrock displacement $r_b(t)$ is governed by the differential equation

$$\ddot{r}_0 + 2\zeta_0\omega_0\dot{r}_0 + \omega_0^2 r_0 = -\ddot{r}_b(t) \tag{17}$$

3 modes are maintained in the expansion of external degrees-of-freedom at system reduction. The modal damping ratios are taken as $\zeta_i = 0.05,\ i = 1,2,3$. The eigenperiods $T_j(t)$ are calculated with an interval of 0.24 $T_1(0)$, using a Rayleigh-Ritz method with the first 5 linear eigenmodes of the innitial undamaged structure as shape functions in combination with Jacobi iteration. Moving time-averages $\hat{T}_j(t)$ of the instantaneous eigenperiods are calculated using an averaging interval of $2.4T_1(0)$.

In the earthquake model only the intensity parameter β_0 of the earthquake process and the angular eigenfrequency ω_0 of the Kanai-Tajimi filter is varied. Below $\beta_{0,i}$ signifies the intensity of the ith earthquake in the sequence. The values ω_0=8.8s^{-1} and ω_0=27.8 s^{-1} are considered for ω_0, which implies resonance in respectively the 1st and the 2nd mode, as the angular eigenfrequencies of the structure are diminishing from their initial values due to the stiffness deterioration of the structure. In all cases a damping ratio of $\zeta_0 = 0.3$ of the Kanai-Tajimi filter is applied. The other parameters used in earthquake generation are $t_1 = 3$ s, $t_0 = 20$ s and $c = 0.2$ s^{-1}. $\beta_0 = 0.6\text{m/s}^{\frac{3}{2}}$, ω_0=8.8 s^{-1} corresponds approximately to a peak surface acceleration of 0.5 g.

Conditional mean values $E[D_{0,3} \mid d_{0,2}, d_{0,1}]$ and conditional variational coefficients $V[D_{0,3} \mid d_{0,2}, d_{0,1}]$ in the 3rd earthquake are estimated for the one-dimensional damage indicator for different observations of $D_{0,1} = d_{0,1}$ in the first earthquake, but for same or close observations of $D_{0,2} = d_{0,2}$ in the second earthquake. Similarly, conditional mean values $E[D_{j,3} \mid \mathbf{d}_2, \mathbf{d}_1], j = 1,2$, conditional variational coefficients $V[D_{j,3} \mid \mathbf{d}_2, \mathbf{d}_1], j = 1,2$ and conditional correlation coefficients $\rho[D_{1,3}, D_{2,3} \mid \mathbf{d}_2, \mathbf{d}_1]$ in the 3rd earthquake are estimated for the two-dimensional damage indicator for different observations of $\mathbf{D}_1 = \mathbf{d}_1$ in the first earthquake and same or close observations of $\mathbf{D}_2 = \mathbf{d}_2$ in the second earthquake. In all cases conditional moment estimates are based on 100 independent simulations. A remarkable observation is, that $\rho[D_{0,i}, D_{1,i} \mid \mathbf{d}_{i-1}, \ldots, \mathbf{d}_1] = 1.000$ in all analysed cases, independently of the damage history. $D_{0,3}$ and $D_{1,3}$ can consequently be assumed to be proportional.

Table 1 and 2 show the obtained conditional moments in the 3rd earthquake for the one-dimensional and two-dimensional damage indicator, respectively. In all cases $d_{0,2} \approx 0.444$, whereas $d_{0,1}$ is varied. The intensities of the earthquakes follow from the legend of the tables. The angular eigenfrequency of the Kanai-Tajimi filter is ω_0 =8.8 s^{-1}, corresponding to resonance in the first mode.

No attempt is made to keep $\mathbf{d}_2^T = [d_{1,2}, d_{2,2}]$ in the second column of Table 2 constant. These values show relatively high variability, which is due to the weaker correlation between $D_{1,2}$ and $D_{2,2}$ ($\rho[D_{1,2}, D_{2,2}] \approx 0.94$). Mean value and variational coefficient of the 15 indicated data in Table 1 for $E[D_{0,3}]$ are $E[E[D_{0,3}]] = 0.6635$ and $V[E[D_{0,3}]] = 0.0362$. If the results of Table 1 at which $d_{2,2}$ values in Table 2 differ significantly from the others are filtered out (these are the rows 4, 6, 7, 8, 13, 14), the corresponding results become $E[E[D_{0,3}]] = 0.6447$ and $V[E[D_{0,3}]] = 0.0253$. The 30 per cent decreases in the variational coefficient of $E[D_{0,3}]$ implies that conditioning on $D_{0,2}$ and $D_{2,2}$ will improve the Markov property of the mean of $D_{0,3}$, compared to conditioning solely on $D_{0,2}$. Surely, the same compaction is observed for the variational coefficient of $E[D_{1,3}]$, since $D_{0,3}$ and $D_{1,3}$ are perfectly correlated. When $V[D_{0,3}]$ is subjected to the same filtering, there is 9 per cent compaction in $V[V[D_{0,3}]]$, which implies that there is also improvement in the Markov property of the variance of $D_{0,3}$.

Similar comparative analysis for the data in Table 1 at which $d_{0,2} = 0.444$ (rows 2, 3, 4, 5, 6, 7, 9, 10, 11 of Table 1) subjected to filtering out the rows 4, 6 and 7 at which the $D_{2,2}$ value differs significantly from the others, shows 50 per cent compaction in $V[E[D_{0,3}]]$ and 13 per cent increase in $V[V[D_{0,3}]]$. This implies that the Markov property of the mean of $D_{0,3}$ has been improved based on such conditioning, whereas the Markov property of the variance has debased. However, the latter observation is quite unique in the material, and is believed to be attributed to statistical scatter due to the very small sample size considered.

When the data in Table 1 at which $d_{0,2} = 0.445$ (rows 1, 8, 12, 13, 14, 15 of Table 1) is analysed similarly (rows 8 and 13 are filtered out), the corresponding results show 45 per cent compaction in $V[E[D_{0,3}]]$ and 9 per cent compaction in $V[V[D_{0,3}]]$, which implies that conditioning on $D_{0,2}$ and $D_{2,2}$ will improve the Markov property of both the mean and the variance of $D_{0,3}$ compared to conditioning solely on $D_{0,2}$.

Table 3 and Table 4 show corresponding results, when the angular eigenfrequency of the Kanai-Tajimi filter is $\omega_0 = 27.8\ \mathrm{s}^{-1}$, corresponding to resonance in the second mode. The intensities of the earthquakes have been increased in order to obtain comparable damage levels.

$E[D_{0,3}]$ and $V[D_{0,3}]$ in Table 3 display the same tendency as the corresponding results in Table 1. In Table 4 major differences compared to Table 2 are that the $d_{2,2}$ values have become more variable, $E[D_{2,3}]$ has increased slightly in proportion to $E[D_{1,3}]$, and the correlation coefficient of $D_{1,3}$ and $D_{2,3}$ has decreased to $\rho[D_{1,3}, D_{2,3}] \approx 0.88$. All these effects are due to the increased excitation of the second mode, which will induce relatively higher damage in the upper part of the building compared to the first mode.

The mean value and the variational coefficient of the 15 results indicated in Table 3 for $E[D_{0,3}]$ are $E[E[D_{0,3}]] = 0.6132$ and $V[E[D_{0,3}]] = 0.0361$. If the data of Table 3 at which $d_{2,2}$ values in Table 4 differ significantly from the others are filtered out (these are the rows 2, 4, 5, 6, 7, 15), the corresponding results become $E[E[D_{0,3}]] = 0.6125$ and $V[E[D_{0,3}]] = 0.0308$. This shows 20 per cent compaction in $V[E[D_{0,3}]]$, which implies that conditioning on $D_{0,2}$ and $D_{2,2}$ will improve the Markov property of the mean of $D_{0,3}$ compared to conditioning solely on $D_{0,2}$. When $V[D_{0,3}]$ is subjected to same filtering, there is 40 per cent compaction in $V[V[D_{0,3}]]$, which implies that there is also improvement in the Markov property of the variance of $D_{0,3}$.

Similar analysis for the data in Table 3 at which $D_{0,2} = 0.442$ (rows 1, 2, 4, 7, 8, 14, 15 of Table 3) with filtering out rows 2,4,7 and 15 shows 95 per cent compaction in $V[E[D_{0,3}]]$ and 30 per cent compaction in $V[V[D_{0,3}]]$, which implies that conditioning on $D_{0,2}$ and

$D_{2,2}$ will improve the Markov property of both the mean and variance of $D_{0,3}$, compared to conditioning solely on $D_{0,2}$.

When the data in Table 3 at which $D_{0,2} = 0.444$ (rows 3, 5, 6, 11, 13 of Table 3), with filtering out rows 5 and 6, are analysed, the corresponding results show 20 per cent compaction in $V[E[D_{0,3}]]$ and 50 per cent compaction in $V[V[D_{0,3}]]$, which again implies that conditioning on $D_{0,2}$ and $D_{2,2}$ will improve the Markov property of the mean and variance of $D_{0,3}$ relative to conditioning solely on $D_{0,2}$.

For the cases studied, conditioning on $D_{1,2}$ and $D_{2,2}$ reduces the variability of the observed mean values and of the observed variational coefficients of $D_{0,3}$ compared to conditioning solely on $D_{0,2}$. Further, this observation has been supported by a number of similar investigations not reported in this paper. Due to the proportionality of $D_{0,i}$ and $D_{2,i}$ it can then be concluded that the Markov properties of the mean and covariances of $[D_{1,i}, D_{2,i}]$ are superior to the Markov property of the mean and variances of the one-dimensional damage indicator $D_{0,i}$.

1st earthquake $d_{0,1}$	2nd earthquake $d_{0,2}$	3rd earthquake $E[D_{0,3}]$	3rd earthquake $V[D_{0,3}]$
0.000	0.445	0.690	0.138
0.201	0.444	0.634	0.124
0.201	0.444	0.654	0.118
0.201	0.444	0.708	0.121
0.235	0.444	0.652	0.131
0.235	0.444	0.623	0.117
0.256	0.444	0.646	0.123
0.257	0.445	0.665	0.153
0.308	0.444	0.666	0.131
0.309	0.444	0.670	0.127
0.309	0.444	0.662	0.112
0.309	0.445	0.664	0.111
0.309	0.445	0.631	0.130
0.310	0.445	0.697	0.132
0.445	0.445	0.690	0.138

Table 1: Damage history, conditional mean value and conditional variational coefficient of one-dimensional maximum softening after 3rd earthquake. $\beta_{0,1}$=0.2 $m/s^{\frac{3}{2}}$, $\beta_{0,2}$=0.2 $m/s^{\frac{3}{2}}$, $\beta_{0,3}$=0.4 $m/s^{\frac{3}{2}}$, ω_0 =8.8 s^{-1}.

1st earthquake $d_{1,1}$	$d_{2,1}$	2nd earthquake $d_{1,2}$	$d_{2,2}$	3rd earthquake $E[D_{1,3}]$	$E[D_{2,3}]$	3rd earthquake $V[D_{1,3}]$	$V[D_{2,3}]$	3rd earthquake $\rho[D_{1,3},D_{2,3}]$
0.000	0.000	0.470	0.226	0.710	0.406	0.128	0.228	0.874
0.215	0.130	0.470	0.224	0.656	0.366	0.115	0.182	0.894
0.214	0.129	0.472	0.222	0.677	0.383	0.110	0.195	0.844
0.214	0.129	0.470	0.229	0.727	0.429	0.112	0.235	0.849
0.252	0.140	0.467	0.224	0.669	0.383	0.122	0.208	0.880
0.251	0.144	0.470	0.219	0.645	0.366	0.109	0.159	0.951
0.274	0.153	0.469	0.234	0.667	0.382	0.114	0.224	0.892
0.272	0.168	0.470	0.234	0.686	0.391	0.142	0.245	0.931
0.328	0.187	0.470	0.219	0.687	0.388	0.121	0.205	0.932
0.331	0.164	0.470	0.225	0.682	0.396	0.104	0.159	0.898
0.331	0.164	0.473	0.226	0.685	0.381	0.103	0.171	0.893
0.331	0.164	0.472	0.220	0.688	0.392	0.118	0.196	0.883
0.331	0.164	0.469	0.227	0.657	0.376	0.120	0.202	0.899
0.332	0.168	0.472	0.230	0.721	0.419	0.123	0.217	0.861
0.470	0.226	0.470	0.226	0.710	0.406	0.128	0.228	0.874

Table 2: Damage history, conditional mean values, conditional variational coefficients and conditional correlation coefficient of two-dimensional maximum softening after 3rd earthquake. $\beta_{0,1}$=0.2 m/s$^{\frac{3}{2}}$, $\beta_{0,2}$=0.2 m/s$^{\frac{3}{2}}$, $\beta_{0,3}$=0.4 m/s$^{\frac{3}{2}}$, ω_0 =8.8 s^{-1}.

1st earthquake $d_{0,1}$	2nd earthquake $d_{0,2}$	3rd earthquake $E[D_{0,3}]$	3rd earthquake $V[D_{0,3}]$
0.000	0.442	0.636	0.142
0.000	0.442	0.643	0.140
0.221	0.444	0.603	0.132
0.228	0.442	0.598	0.112
0.300	0.444	0.587	0.107
0.300	0.444	0.581	0.105
0.307	0.442	0.633	0.144
0.307	0.442	0.637	0.125
0.307	0.443	0.613	0.145
0.332	0.443	0.584	0.132
0.332	0.444	0.590	0.121
0.332	0.443	0.603	0.141
0.333	0.444	0.611	0.137
0.442	0.442	0.636	0.142
0.442	0.442	0.643	0.140

Table 3: Damage history, conditional mean value and conditional variational coefficient of one-dimensional maximum softening after 3rd earthquake. $\beta_{0,1}$=0.3 m/s$^{\frac{3}{2}}$, $\beta_{0,2}$=0.3 m/s$^{\frac{3}{2}}$, $\beta_{0,3}$=0.5 m/s$^{\frac{3}{2}}$, ω_0 =27.8 s^{-1}.

1st earthquake $d_{1,1}$	$d_{2,1}$	2nd earthquake $d_{1,2}$	$d_{2,2}$	3rd earthquake $E[D_{1,3}]$	$E[D_{2,3}]$	3rd earthquake $V[D_{1,3}]$	$V[D_{2,3}]$	3rd earthquake $\rho[D_{1,3}, D_{2,3}]$
0.000	0.000	0.467	0.230	0.657	0.380	0.132	0.232	0.876
0.000	0.000	0.466	0.258	0.663	0.402	0.132	0.194	0.836
0.235	0.141	0.469	0.229	0.625	0.365	0.123	0.194	0.856
0.240	0.162	0.468	0.224	0.620	0.357	0.105	0.183	0.890
0.321	0.165	0.470	0.222	0.609	0.357	0.100	0.146	0.875
0.321	0.165	0.470	0.221	0.603	0.356	0.099	0.156	0.842
0.327	0.175	0.468	0.216	0.654	0.378	0.135	0.200	0.891
0.327	0.179	0.468	0.228	0.658	0.380	0.117	0.196	0.913
0.327	0.179	0.469	0.234	0.634	0.386	0.136	0.180	0.892
0.352	0.200	0.468	0.231	0.606	0.363	0.123	0.179	0.896
0.352	0.200	0.469	0.239	0.612	0.363	0.113	0.173	0.883
0.352	0.200	0.469	0.232	0.625	0.369	0.132	0.181	0.898
0.355	0.187	0.470	0.232	0.632	0.381	0.146	0.214	0.900
0.467	0.230	0.467	0.230	0.657	0.380	0.132	0.232	0.876
0.466	0.258	0.466	0.258	0.663	0.402	0.132	0.194	0.836

Table 4: Damage history, conditional mean values, conditional variational coefficients and conditional correlation coefficient of two-dimensional maximum softening after 3rd earthquake. $\beta_{0,1}$=0.3 m/s$^{\frac{3}{2}}$, $\beta_{0,2}$=0.3 m/s$^{\frac{3}{2}}$, $\beta_{0,3}$=0.5 m/s$^{\frac{3}{2}}$, ω_0 =27.8 s^{-1}.

6. CONCLUSIONS

In this study, a one dimensional scalar valued and a two-dimensional vector valued maximum softening damage indicator are defined. The one-dimensional damage indicator, defined considering the variation in the first period of the structure, analogous to a SDOF system, is a genuine global damage index representing the average damage throughout the whole structure. The two-dimensional damage indicators are defined considering the variations in the first and second periods of the structure, and thus is analogous to an equivalent linear two degree-of-freedom system. The components of the two dimensional damage vector can be interpreted as damage indicators for the lower half and the upper half of the structure, hence representing a simple and crude local description of the damage state of the structure.

Since statements on the post earthquake reliability should be obtained solely from knowledge of the latest recorded values of the damage indicators above defined, these damage indicators are required to possess Markov property. This problem has been investigated based on numerical Monte-Carlo simulations. A sample plane frame which has been designed according to the UBC specifications for earthquake zone 4 is subjected to realizations of different earthquakes and the value of the damage indicators is obtained using the computer program SARCOF. For the studied cases, it is observed that the Markov assumption of the one-dimensional damage indicator is justified for the mean value of the transition probability density function (tpdf), whereas some deviations are observed for the variance and higher order statistical moments. Tests checking whether conditioning on two dimensional damage vector improves Markov property of the one-dimensional damage indicator demonstrated that the Markov properties of the mean and covariances of the two-dimensional indicators are superior to the Markov property of the first and second order moments of the one-dimensional damage indicator.

Finally following the results of this study, it is expected that the Markov property of n dimensional damage indicators should have better Markov property compared to the $n-1$ dimensional ones.

7. REFERENCES

1 Cecen, H. (1979): *Response of ten story, reinforced concrete model frames to simulated earthquakes.* Ph.D.-thesis. University of Illinois at Urbana Champaign.

2 DiPasquale, E. and Cakmak, A.S. (1987): *Detection and Assessment of Structural Damage.* Technical Report NCEER-87-0015, National Center for Earthquake Engineering Research, State University of New York at Buffalo.

3 DiPasquale, E. and Cakmak, A.S. (1989): *On the derivation between local and global damage indices.* Technical Report NCEER-89-0034, National Center for Earthquake Engineering Research, State University of New York at Buffalo.

4 DiPasquale, E. and Cakmak, A.S. (1990): *Detection of Seismic Structural Damage Using Parameter-Based Global Damage Indices.* Probabilistic Engineering Mechanics, Vol. 5, 60-65.

5 Healey, T.J. and Sozen, M.A. (1978): *Experimental study of the dynamic response of a ten story reinforced concrete frame with a tall first story.* Report No. UILU-ENG-78-2012, SRS 450, University of Illinois at Urbana-Champaign.

6 Jennings, P.C., Housner, G.W. and Tsai, N.C. (1968): *Simulated Earthquake Motions.* Report of the Earthquake Engineering Research Laboratoria, California Institute of Technology.

7 Mørk, K.J. (1992) : *Stochastic Analysis of Reinforced Concrete Frames under Seismic Excitation.* Soil Dynamics and Earthquake Engineering, Vol. 11, No. 3, xx-yy.

8 Nielsen, S.R.K. and Cakmak, A.S. (1991): *Evaluation of Maximum Softening as a Damage Indicator for Reinforced Concrete Under Seismic Excitation.* Proc. 1st Int. Conf. on Computational Stochastic Mechanics, ed. Spanos, P.D. and Brebbia, C.A., 169-184.

9 Rodriguez-Gomez, S. (1990): *Evaluation of Seismic Damage Indices for Reinforced Concrete Structures.* M.Sc.Eng. Dissertation. Department of Civil Engineering and Operations Research, Princeton University, Princeton, N.J.

10 Rodriguez-Gomez, S., Chung,Y.S. and Meyer, C. (1990): *SARCF-II User's Guide. Seismic Analysis of Reinforced Concrete Frames.* Technical Report NCEER-90-0027, National Center for Earthquake Engineering Research, State University of New York at Buffalo.

11 Roufaiel, M.S.L. and Meyer, C. (1987): *Analytical Modeling of Hysteretic Behaviour of R/C Frames.* J. Struct. Engng., ASCE, Vol. 113, 429-444.

12 Ruiz, P. and Penzien, J. (1969): *Probabilistic Study of Behavior of Structures during Earthquakes.* Report No. EERC 69-3, University of California, Berkeley, Cal.

13 Tajimi, H. (1960): *Semi-empirical Formula for the Seismic Characteristics of the Ground.* Proceedings of the 2nd World Conference on Earthquake Engineering, Vol. II, 781-798, Tokyo and Kyoto.

14 Uniform Building Code (1988): *Earthquake Regulations.*

STRUCTURAL RELIABILITY THEORY SERIES

PAPER NO. 62: S. R. K. Nielsen, P. Thoft-Christensen, K. J. Mørk: *Reliability of Hysteretic Systems Subjected to White Noise Excitation.* ISSN 0902-7513 R8916.

PAPER NO. 63: S. R. K. Nielsen, P. Thoft-Christensen, H. Moust Jacobsen: *Reliability of Soil Sublayers Under Earthquake Excitation: Markov Approach.* ISSN 0902-7513 R8917.

PAPER NO. 64: M. V. Delmar, J. D. Sørensen: *Reliability of Elasto-Plastic Structural Systems.* ISSN 0902-7513 R8932.

PAPER NO. 65: J. D. Sørensen, P. Thoft-Christensen: *Reliability-Based Optimization of Parallel Systems.* ISSN 0902-7513 R8930.

PAPER NO. 66: R. Iwankiewics, S. R. K. Nielsen: *Dynamic Response of Non-Linear Inelastic Systems to Poisson-Driven Stochastic Excitations.* ISSN 0902-7513 R8931.

PAPER NO. 67: J. D. Sørensen & P. Thoft-Christensen: *Reliability of Structural Systems with Regard to Permanent Displacements.* ISSN 0902-7513 R9017.

PAPER NO. 68: R. Iwankiewicz, S. R. K. Nielsen: *Probability Density of The Response of Dynamic Systems to Poisson-Distributed Random Impulses.* ISSN 0902-7513 R9109.

PAPER NO. 69: J. D. Sørensen, Ib Enevoldsen: *Sensitivity Analysis in Reliability-Based Shape Optimization.* ISSN 0902-7513 R8924.

PAPER NO. 70: P. Thoft-Christensen: *On Reliability-Based Optimal Design of Structures.* ISSN 0902-7513 R9019.

PAPER NO. 71: K. J. Mørk & S. R. K. Nielsen: *Reliability of Soil Sublayers under Earthquake Excitation.* ISSN 0902-7513 R9005.

PAPER NO. 72: G. Sigurdsson & S. R. K. Nielsen: *Stress Response of Offshore Structures by Equivalent Polynomial Expansion Techniques.* ISSN 0902-7513 R9014.

PAPER NO. 73: I. Enevoldsen, J. D. Sørensen & G. Sigurdsson: *Reliability-Based Shape Optimization Using Stochastic Finite Elements.* ISSN 0902-7513 R9013.

PAPER NO. 74: A. M. Sommer & P. Thoft-Christensen: *Inspection and Maintenance of Marine Steel Structures - State-of-the-Art.* ISSN 0902-7513 R9012.

PAPER NO. 75: F. M. Jensen & P. Thoft-Christensen: *Optimization of Large, Complex Structures - An Overview.* ISSN 0902-7513 R9016.

PAPER NO. 76: Kim J. Mørk & Søren R. K. Nielsen: *System Reduction for Random Dynamically loaded Elasto-Plastic Structures.* ISSN 0902-7513 R9029.

PAPER NO. 77: G. B. Pirzada & P. Thoft-Christensen: *Beta-Unzipping of Plastic Slabs at Mechanism Level.* ISSN 0902-7513 R9033.

STRUCTURAL RELIABILITY THEORY SERIES

PAPER NO. 78: Ib Enevoldsen & J. D. Sørensen: *Optimization Algorithms for Calculation of the Joint Design Point in Parallel Systems.* ISSN 0902-7513 R9032.

PAPER NO. 79: F. M. Jensen & P. Thoft-Christensen: *Reliability-Based Structural Optimization Using Linear Decomposition Technique.* ISSN 0903-7513 R9101.

PAPER NO. 80: A. M. Sommer, A. S. Nowak & P. Thoft-Christensen: *Inspection Strategies for Highway Steel Girder Bridges.* ISSN 0902-7513 R9102.

PAPER NO. 81: S. R. K. Nielsen: *Probability of Failure by Integral Equation Methods.* ISSN 0902-7513 R9037.

PAPER NO. 82: I. Enevoldsen & J. D. Sørensen: *Reliability-Based Optimization of Series Systems of Parallel Systems.* ISSN 0902-7513 R9039.

PAPER NO. 83: S. R. K. Nielsen & A. S. Cakmak: *Evaluation of Maximum Softening as a Damage Indicator for Reinforced Concrete under Seismic Excitation.* ISSN 0902-7513 R9048.

PAPER NO. 84: G. B. Pirzada: *Estimation of the Reliability of Plastic Slabs.* Ph.D.-Thesis. ISSN 0902-7513 R9049.

PAPER NO. 85: A. Johansen & P. Thoft-Christensen: *Estimation of the Reliability of Existing Structures - An Overview.* ISSN 0902-7513 R9140.

PAPER NO. 86: J. Almlund: *Life Cycle Model for Offshore Installations for Use in Prospect Evaluation.* Ph.D.-Thesis. ISSN 0902-7513 R9139.

PAPER NO. 87: I. Enevoldsen: *Reliability-Based Structural Optimization.* Ph.D.-Thesis. ISSN 0902-7513 R9106.

PAPER NO. 88: J. D. Sørensen & M. H. Faber: *Optimal Inspection and Repair Strategies.* ISSN 0902-7513.

PAPER NO. 89: M. Delmar & J. D. Sørensen: *Probabilistic Analysis in Economic Decision Making.* ISSN 0902-7513 R9153.

PAPER NO. 91: K. J. Mørk & S. R. K. Nielsen: *Program for Stochastic Analysis of Plane Reinforced Concrete Frames under Seismic Excitation.* ISSN 0902-7513 R9129.

PAPER NO. 92: S. R. K. Nielsen, H. U. Köylüoğlu & A. Ş. Çakmak: *One and Two-Dimensional Maximum Softening Damage Indicators for Reinforced Concrete Structures under Seismic Excitation.* ISSN 0902-7513 R9211.

PAPER NO. 99: K. J. Mørk: *Stochastic Response Analysis of 3D Reinforced Concrete Structures under Seismic Excitation.* ISSN 0902-7513 R9209.

Department of Building Technology and Structural Engineering
University of Aalborg, Sohngaardsholmsvej 57. DK 9000 Aalborg
Telephone: 45 98 15 85 22 Telefax: 45 98 14 82 43